

## Sol-gel Synthesis, Structural and Characterization of Ag-Gd-Ti-O Nanocomposites†

S. RAMESH<sup>1,2,\*</sup> and B.B. DAS<sup>2</sup>

<sup>1</sup>Department of Science and Humanities, Saveetha School of Engineering, Saveetha University, Chennai-602 105, India

<sup>2</sup>Department of Chemistry, School of Physical, Chemical and Applied Sciences, Pondicherry University, Pondicherry-605 014, India

\*Corresponding author: E-mail: rameshsiva\_chem@yahoo.com

AJC-11690

The  $\text{Ag}_{3(2+x)}\text{Gd}_x\text{Ti}_{4-x}\text{O}_{11+\delta}$  ( $0.0 \leq x \leq 1.0$ ) ( $x = 0, 0.25, 0.5, 0.75$  and  $1.0$ ) nanocomposites were successfully synthesized by sol-gel technique. The surface morphology, structure and the properties of nanocomposites were investigated by SEM, XRD, UV, EPR and VSM. The XRD result reveals that the composites were formed in tetragonal lattice type with P42/nm space group. The average crystallite size of the composites varied from 44 nm to 63 nm. The surface morphology of the samples was evaluated by SEM. The purity of the composites was confirmed through the energy dispersive X-ray analysis. Electron paramagnetic resonance line shapes were recorded at 8, 77 and 300 K, which are isotropic in nature. The magnetic susceptibility values of the samples are in ferromagnetic nature at room temperature.

**Key Words:** Composite materials, Sol-gel processes, Electron paramagnetic resonance, X-ray diffraction.

### INTRODUCTION

In recent years, much attention has been paid on rare earth (RE) containing transition metal ions (TM) nanocomposites. This is due to various reasons, in the materials chemist point of view these materials provides valuable information about basic phenomena like cluster formation and interaction, quantum confinement effects, *etc.* However, the application point of view the  $4f$ - $3d$  complexes were used in several fields<sup>1</sup> such as optical lasers<sup>2</sup>, up-conversion luminescence for colour displays<sup>3</sup>, high density optical data reading and storage super-conductor magnetic materials<sup>4</sup> medical, *etc.* This is due to extremely high melting points of rare-earth metal ions and transition metal oxides. Recently, chemists pay more attention on  $\text{Pr}^{3+}$ ,  $\text{Nd}^{3+}$ ,  $\text{Er}^{3+}$  and  $\text{Gd}^{3+}$  doped transition metal compounds because these materials can be used in the visible spectral region at room temperature. Considering the high coordination number of  $\text{RE}^{3+}$  may render the structural flexibility and increase the stability of the  $\text{RE}^{3+}$  doped transition metal composites. The host materials are playing a vital role in developing the rare-earth-doped transition metal composites. The researchers are mainly focused on silicates and oxides that are more suitable for practical applications due to their high chemical durability and thermal stabilities. In the modern research aimed ferromagnetic wide band gap semiconductors with a Curie temperature at above 300 K. Doping the rare

earth elements are having a better promising alternative to transition metal. The rare earth atoms are having partially filled  $f$ -orbitals, which carries magnetic moments and it can take part in magnetic coupling as in the case of partially field  $d$  orbitals in the transition metals atoms. Among all the rare earth ions  $\text{Gd}^{3+}$  ion is the only element has both partially filled  $4f$  and  $5d$  orbitals this can lead a new coupling mechanism *via* intra ion  $4f$ - $5d$  exchange interaction followed by inter-ion  $5d$ - $5d$  coupling mediated by charge carriers. The ferromagnetism in  $\text{Gd}^{3+}$  doped ternary alloy Ga-Gd-N films has been observed with a Curie temperature of 400 K. There are only a few investigations about the electronic structures and spectroscopic parameters of  $\text{Gd}^{3+}$  in crystals and glasses.

In this report, we describe the sol-gel synthesis and structure-property relations in  $\text{Ag}_{3(2+x)}\text{Gd}_x\text{Ti}_{4-x}\text{O}_{11+\delta}$  ( $x = 0, 0.25, 0.5, 0.75, 1.0$ ) nanocomposites using various experimental techniques.

### EXPERIMENTAL

Sol-gel method has been used to prepare the  $\text{Ag}_{3(2+x)}\text{Gd}_x\text{Ti}_{4-x}\text{O}_{11+\delta}$  ( $x = 0, 0.25, 0.5, 0.75, 1.0$ ) nanocomposites. All the reagent grade chemicals were used as received as without further purification. Calculated amounts of  $\text{Gd}_2\text{O}_3$ ,  $\text{AgNO}_3$  and  $\text{TiO}_2$  were mixed together in 2 M nitric acid medium by stirring for 1 h at pH - 4-5, followed by the addition of 30 mL of 1.5 M citric acid solution this was stirred continuously at 60 °C

†Presented at International Conference on Global Trends in Pure and Applied Chemical Sciences, 3-4 March, 2012; Udaipur, India

TABLE-1  
LATTICE PARAMETERS, DENSITY VALUES AND CHEMICAL ANALYSIS RESULTS  
OF A1-A5 OF  $\text{Ag}_{3(2+x)}\text{Gd}_x\text{Ti}_{4-x}\text{O}_{11+\delta}$  ( $0 \leq x \leq 1.0$ ) NANOCOMPOSITES

S. No	a(Å)	b(Å)	c(Å)	Unit cell volume (Å <sup>3</sup> )	Density (g/cm <sup>3</sup> )	No. of Ti <sup>3+</sup> ions per g	Crystallite size (nm)
A1	7.7535	7.7535	9.1661	551.04	2.772	$5.321 \times 10^{20}$	48
A2	7.2536	7.2536	10.5365	554.38	2.300	$2.940 \times 10^{19}$	54
A3	6.8565	6.8565	10.1635	477.80	2.969	$2.766 \times 10^{20}$	57
A4	8.0475	8.0475	6.3109	408.71	3.247	$1.793 \times 10^{20}$	48
A5	7.0764	7.0764	8.0492	403.06	4.890	$1.394 \times 10^{20}$	63

Crystal system: Tetragonal; Space group: P42/nmm

until it becomes the transparent gel. Then the gel was dried using an air oven at 200 °C for 1 h. This process leads to the formation of light weight porous materials due to the enormous amount of gas evolution and finally it was sintered at 850 °C for 4 h to get the fine homogeneous dense powder. The powder X-ray diffraction patterns of the samples were identified by using a X'Pert (PANalytical) powder X-ray diffractometer. Monochromatic  $\text{CuK}\alpha$  radiation was used as a source with 40 kV/30 mA power. The SEM images were recorded by using Hitachi-S3400 instrument and EDX was done by a SUPER DRYER II instrument. The concentrations of Ti<sup>3+</sup> ions were determined by wet chemistry and the densities were determined by liquid displacement method. The X-band EPR spectral data at 300 and 77 K were recorded with a JEOL JES-TE 100 ESR spectrometer and 13 K were recorded on a Varian EPR spectrometer. The optical absorption spectra were recorded by a Varian Cary 5000 UV-VIS-NIR spectrometer in the solid phase. The magnetic moments data were recorded on a LAKESHORE VSM 7404 vibrating sample magnetometer.

## RESULTS AND DISCUSSION

The powder XRD patterns of the sol gel synthesized  $\text{Ag}_{3(2+x)}\text{Gd}_x\text{Ti}_{4-x}\text{O}_{11+\delta}$  ( $0.0 \leq x \leq 1.0$ ; A1-A5) samples are shown in Fig. 1. In the diffraction patterns, all the major peaks were appeared at the same diffraction angle which shows that the samples (A1-A5) are formed in single phase polycrystalline materials. All the diffraction patterns were indexed perfectly using the least square method to avoid the difference between the experimental and theoretical pattern. Further structural information was carried by Rietveld refinements analysis with the FullProf software package 2003. The refinement result reveals that all the composites are formed in single phase Tetragonal lattice with P42/nmm (Space group no 134) space group. This is in good agreement with the standard values. The lattice type and the space group were found to be remaining constant and the Gd<sup>3+</sup> ion incorporation did not give any structural and the phase changes of the samples within the atomic concentration range ( $0.0 \leq x \leq 1.0$ ) studied possibly due to the very low concentration of the Gd<sup>3+</sup> ion present in the host lattice. The calculated lattice parameters of the composites are given in Table-1.

Average crystallite size of the composites were calculated from the full width at half maximum (FWHM) of all the peaks using the Debye-Scherrer relation and Williamson-Hall equation. Here, as vary the composition ratio the average size of the particle is varied from 44 (A1) to 63 nm (A5) are shown in Table-1. The crystallite sizes of the samples are increasing with respect to the increasing content of the Gd<sup>3+</sup> ions. The crystallite size is gradually increasing due to the higher ionic

radius of Gd<sup>3+</sup> (2.54 Å) replaced by smaller Ti<sup>3+</sup> (2.0 Å) ions it increases the bond length in the crystal structure.

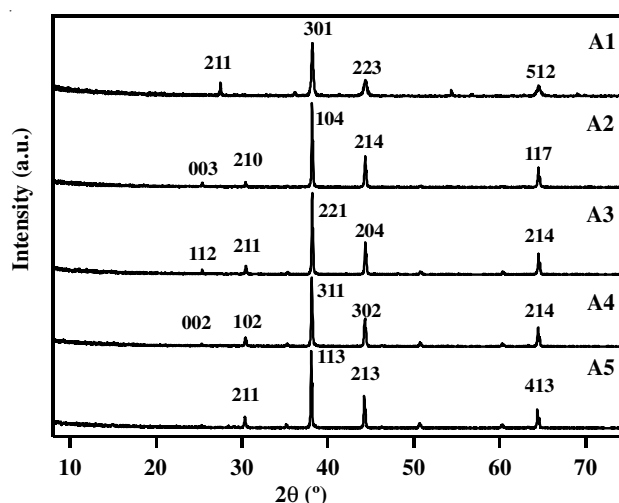


Fig. 1. Powder X-ray diffraction pattern of A1-A5 of  $\text{Ag}_{3(2+x)}\text{Gd}_x\text{Ti}_{4-x}\text{O}_{11+\delta}$  ( $0 \leq x \leq 1.0$ ) nanocomposites

The concentrations of Ti<sup>3+</sup> ions were determined by wet chemistry method. The value of the Ti<sup>3+</sup> ions are gradually decreased as we expect from the composition ratio this proved that the particular composition of the samples is formed. The densities of the samples were obtained using liquid displacement method (experimental) and also from the lattice parameters (calculated). The densities of the samples are gradually increases from A1-A5 with increasing content of the Gd<sup>3+</sup> ionic concentration this may be due to the higher density of the Gd increases. The densities of the samples were obtained from the powder XRD analysis is coincides with experimental values. This is another evidence of the powder XRD refinement analysis which is in good agreement with the standard values.

In order to examine the quantitative analysis and distribution of metal ions of randomly selected  $\text{Ag}_{3(2+x)}\text{Gd}_x\text{Ti}_{4-x}\text{O}_{11+\delta}$  nanocomposites at different magnification were performed by SEM-EDX analysis. Fig. 2. Shows the (a) SEM micrographs of A1, A3 and A5 along with (b) energy dispersive X-ray (EDX) profile (A2) and (c) X-ray mapping of A2. The morphology of the sample A1 shows uneven rod like shape when the Gd ions are incorporated into the samples A2-A5 the samples shows globular in shape. The purity of the samples was confirmed from the EDX profile and quantitative results. The elemental analysis by the EDX results indicates the constituent elements like Ag, Gd, Ti and O are present in the composites. The atomic percentage of the elements were very close to the expected ratio as stated in the synthesis method

and no other extra elements were observed this conforms to the formations of pure  $\text{Ag}_{3(2+x)}\text{Gd}_x\text{Ti}_{4-x}\text{O}_{11+\delta}$  nanocomposites. The X-ray mapping of the composites reveals the presence of all the constituent elements and it is uniformly distributed throughout the surface with resemble of their relative amounts.

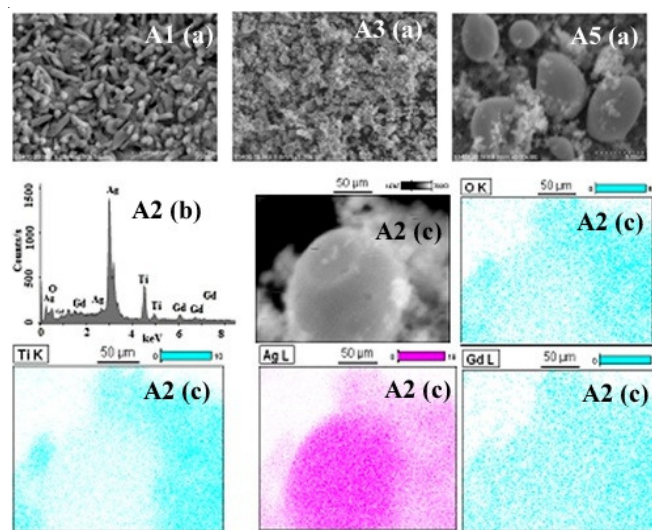


Fig. 2. (a) The SEM morphology (b) EDX- profile of (c) X-ray mapping of  $\text{Ag}_{3(2+x)}\text{Gd}_x\text{Ti}_{4-x}\text{O}_{11+\delta}$  ( $0 \leq x \leq 1.0$ ; A1-A5) nanocomposites

The EPR technique has been widely employed in this composites characterization due to the existence of the EPR active elements such as Ti and Gd are present in this composite. It's a single progress to understand the both electronic and geometrical features of the elements in different chemical environments. The EPR line shapes of the A1-A5 sample shows isotropic lineshapes are centered at  $g=2.01$  at the 300, 77 and 13 K. The EPR lineshapes are mainly arises from the  $\text{Gd}^{3+}$  ( $4f^7$ ) and  $\text{Ti}^{3+}$  ( $d^1$ ) ions. The small extra lines were observed on both sides may be due to the superimposed hyperfine features of  $^{158}\text{Gd}$  ( $I = 3/2$ ) or  $^{47}\text{Ti}$  ( $I = 5/2$ ) isotopes. However, the isotropic exchange interaction usually dominates the effects of the spin-orbit coupling and magnetic dipole interaction of the metal ions. The electron spin resonance of  $\text{Ti}^{3+}$  ( $d^1$ ) and  $\text{Gd}^{3+}$  ( $4f^7$ ) ions has been detected in only at very low temperature due to rapid spin lattice relaxation<sup>5,6</sup>.

The optical absorption spectral bands are appeared at 320, 348 and 523 nm. The bands are assigned with the reported data. It reveals the broad band at 320 nm is attributed to the  $\text{Ti}^{3+}$  ions and the bands at 348 nm corresponds to the presence of Ag-TiO<sub>2</sub> nanoparticles. The same results lead to the samples can be used for photocatalysis<sup>7</sup>. The band at 523 nm is correspond to the f-f transitions of  $\text{Gd}^{3+}$  ions in the crystal lattice, which are attributed to the  $^8S_{7/2} \rightarrow ^6I_7$  transitions of  $\text{Gd}^{3+}$  ions<sup>8</sup>.

The magnetic properties of the samples were studied by vibrating sample magnetometer at room temperature. The magnetization (M) versus magnetic field (H) shows hysteresis loops in all the cases and the shape of the magnetization curves shows the characteristic of weak ferromagnetism. The value of saturation magnetization, coercivity (Hci) and remenance (Mr) are obtained from these curves and it is reported in the Table-2. The magnetic saturation (Ms) of the samples in the hysteresis loops were not saturated even after the magnetic field of  $\pm 10000\text{G}$ .

The hysteresis loops for the Ag-Gd-Ti nanoparticle show coercivity even at room temperature but the value of Hci is considerably smaller than would be predicted from the particle size. The coercivity, remanent decreases and the saturation magnetization increases linearly with increasing the content of the  $\text{Gd}^{3+}$  ions. The hysteresis loops are narrowed without any jerks in the magnetic spins for all the samples this indicates that magnetic spins are attaining a better homogeneous structure in room temperature this can be a another proof of the single phase formation and purity of the nanocomposites. The magnetic susceptibility ( $\chi$ ) and exchange integral (j) were calculated are shown in the Table-2. The fairly high values of the magnetic susceptibilities in the order of  $10^{-4}$  emu/gG show that the specimens are weak ferromagnetic at 300 K. The calculated exchange integral of the order of  $10^{13}$  Hz shows fairly rapid exchange process in the samples. The Weiss constant values do not vary significantly within the composition range studied.

TABLE-2  
OBSERVED VALUES OF g-MATRICES AT 300, 77 AND 8 K AND MAGNETIC SUSCEPTIBILITY, EXCHANGE INTEGRAL OF A1-A5 OF  $\text{Ag}_{3(2+x)}\text{Gd}_x\text{Ti}_{4-x}\text{O}_{11+\delta}$  ( $0 \leq x \leq 1.0$ ) NANOCOMPOSITES

S. No	Hci (G)	Ms (emu)	Mr $\times 10^{-6}$ (emu)	Magnetic susceptibility ( $\chi$ ) emu/gG	Exchange integral (j) (Hz)
A1	52.200	$176.7 \times 10^{-6}$	68.512	$1.71 \times 10^{-4}$	$1.233 \times 10^{13}$
A2	41.311	$1.66 \times 10^{-3}$	13.291	$7.41 \times 10^{-5}$	$1.248 \times 10^{13}$
A3	64.886	$2.46 \times 10^{-3}$	27.586	$5.78 \times 10^{-4}$	$1.248 \times 10^{13}$
A4	31.973	$3.69 \times 10^{-3}$	20.440	$2.24 \times 10^{-4}$	$1.247 \times 10^{13}$
A5	28.623	$4.26 \times 10^{-3}$	17.181	$3.52 \times 10^{-3}$	$1.249 \times 10^{13}$

## Conclusion

The  $\text{Ag}_{3(2+x)}\text{Gd}_x\text{Ti}_{4-x}\text{O}_{11+\delta}$  ( $0.0 \leq x \leq 1.0$ ) nanocomposites was successfully prepared by the sol-gel technique and the structural characterization were studied. The main features of their structure analysis were confirmed by power XRD. It reveals that all the samples are formed in tetragonal lattice with P42/nmm space group. Average crystallize sizes are found to be in the range 44-63 nm. The morphology of the samples shows rod like shape to spherical shape. The EDX results shows all the constituent elements present and are distributed homogenously. The EPR lineshapes of the samples at 300, 77 and 13 K are broadened isotropic in nature with  $g=2.02$ . The magnetic susceptibility  $10^{-4}$  emu/gG shows fairly strong paramagnetic nature of the samples. Exchange integral of the order of  $10^{13}$  fairly rapid exchange process in the samples.

## REFERENCES

- M.C. Yin, X.F. Lei, M. Li, L.J. Yuan and J.T. Sun, *J. Phys. Chem. Solid.*, **67**, 1372 (2006).
- L.P. Lu, X.Y. Zhang, Z.H. Bai and X.C. Wang, *J. Luminescence.*, **131**, 2372 (2011).
- G. Harkonen, M. Leppanen, E. Soininen, R. Tornqvist and J. Viljanen, *J. Alloys Compd.*, **225**, 552 (1995).
- S. Dhar, L. Pérez, O. Brandt, A. Trampert, K.H. Ploog, J. Keller and B. Beschoten, *Phys. Rev. B.*, **72**, 245203 (2005).
- S. Ramesh and B.B. Das, *J. Korean Chem. Soc.*, **55**, 502 (2011).
- M. Yamaga, T. Yosida, B. Henderson, K.P. O'Donnell and M. Date, *J. Phys. Condens. Mater.*, **3**, 7285 (1992).
- X. Zhu, Q. Li, N. Ming and Z. Meng, *Appl. Phys. Lett.*, **71**, 867 (1997).
- B. Han, H. Liang, Y. Huang, Y. Tao and S. Qiang, *J. Phys. Chem. C.*, **114**, 6770 (2010).